Palaeogeography, Palaeoclimatology, Palaeoecology 630 (2023) 111810

Contents lists available at ScienceDirect

Palaeogeography, Palaeoclimatology, Palaeoecology

journal homepage: www.elsevier.com/locate/palaeo

# ENSO-related East Asian climate transition at ~ 3600 B.P. and its implications for the rise of pastoralism in North China

Shaohua Tian [a], Guoqiao Xiao [b,*], Qiuzhen Yin [c], Zongmin Zhu [a]

[a] State Key Laboratory of Biogeology and Environmental Geology, School of Earth Sciences, China University of Geosciences, Wuhan 430074, China
[b] Hubei Key Laboratory of Critical Zone Evolution, School of Geography and Information Engineering, China University of Geosciences, Wuhan 430078, China
[c] Georges Lemaître Center for Earth and Climate Research, Earth and Life Institute, Universite Catholique de Louvain, Louvain-la-Neuve 1348, Belgium

ARTICLE INFO

Editor: Dr. Howard Falcon-Lang

*Keywords*
Late Holocene
Climate degradation
Dipole pattern
Paleo-ENSO
Pastoralism

ABSTRACT

A transition from cereal-based agriculture to pastoralism in North China occurred around 3600 cal yr B.P., and corresponded to Northern Hemisphere cooling and the onset of an arid climate over North China. In this paper, we investigate the mechanisms for the ~3600 cal yr B.P. climate transition that may have triggered this change in Chinese civilization based on a compilation of 33 high-resolution paleoclimate records spanning the 4000–3000 cal yr B.P. interval. Results show that North and South China experienced a meridional dipole pattern of the climate change. From 4000 to 3600 cal yr B.P., the region north of 30°N was wet and the region south of 30°N was dry, then from 3600 to 3000 cal yr B.P., the pattern reversed with a drier north and a wetter south. We found that this climate transition was related to the onset of a more El Niño-like state in the tropical Pacific Ocean after ~3600 cal yr B.P., which resulted in more precipitation in South China but less precipitation in North China. Climate in the marginal monsoon areas of North China deteriorated, becoming more cold and arid, and pastoralism replaced cereal agriculture as the dominant mode of subsistence. Our study highlights the important role of the paleo-El Niño-Southern Oscillation (paleo-ENSO) for the evolution of civilization in China.

## 1. Introduction

Pastoralism plays a vital role in Chinese civilization, significantly influencing its evolution (Shao and Wu, 2020). Originating from cereal agriculture in North China, the primary shift to pastoralism occurred around 3600 cal yr B.P. (Fig. 1). The Qijia culture dominated the Gansu-Qinghai Cultural Region (Fig. 2a) from 4100 to 3600 cal yr B.P. (Wang, 2012; Chen et al., 2015a; Cui et al., 2018; Chen et al., 2020). Initially thriving, cereal agriculture declined during the later stages of the Qijia culture (An et al., 2005). By ~3600 cal yr B.P., the Qijia culture vanished, giving rise to the Kayue culture (3600–2600 cal yr B.P.; Chen et al., 2015a; Chinese Cultural Atlas Editorial Committee of National Cultural Heritage Administration, 2006, 2011), Xindian culture (3400–2600 cal yr B.P.; Xie, 2002; Chen et al., 2020), Nuomuhong culture (3400–2500 cal yr B.P.; Dong et al., 2016), and Siwa culture (3300–2500 cal yr B.P.; Wang, 2012; Liu and Feng, 2012) in the region (Fig. 2b). Unlike the Qijia culture, these emerging cultures primarily operated on a nomadic-based economy (Yang, 1985; Han, 2005; Chinese Cultural Atlas Editorial Committee of National Cultural Heritage Administration, 2006, 2011; Liu and Feng, 2012; Wang, 2012).

The ascent of pastoralism in the Gansu-Qinghai Cultural Region around 3600 cal yr B.P. is corroborated by an upsurge in the total concentration of coprophilous fungal spores (Wei et al., 2021) and amplified grassland degradation due to grazing activities (Huang et al., 2017; Wei et al., 2020) on the Qinghai-Tibet Plateau. In the Southern Inner Mongolia Cultural Region, the transition from cereal agriculture to pastoralism in the Zhukaigou culture (4000–3500 cal yr B.P.) becomes evident in its latter phase, as seen by the rise in the proportion of sheep and cattle bones (Qiao, 1992; Han, 2005). Meanwhile, in the Southeastern Inner Mongolia Cultural Region, the Lower Xiajiadian culture (4200–3500 cal yr B.P.) predominantly operated on cereal agriculture but incorporated significant animal husbandry (Fig. 2c; Shi et al., 2022). In contrast, the succeeding Upper Xiajiadian culture (3200–2500 cal yr B.P.) exhibited marked pastoral tendencies (Fig. 2d), characterized by a decline in crops, a surge in the proportion of sheep and cattle bones, and the emergence of pastoralism-linked veined bronze ware decorations (Tong, 1993; Shelach et al., 2003; Han, 2005; Liu and Feng, 2012; Jia et al., 2016; Shao and Wu, 2020). This archaeological evidence underscores a pivotal shift from cereal agriculture to pastoralism around 3600 cal yr B.P. in North China, spanning from the western Qinghai and

* Corresponding author.
*E-mail addresses:* xgqiaocug@gmail.com, gqxiaocug@126.com (G. Xiao).

https://doi.org/10.1016/j.palaeo.2023.111810
Received 4 June 2023; Received in revised form 8 September 2023; Accepted 8 September 2023
Available online 11 September 2023
0031-0182/© 2023 Elsevier B.V. All rights reserved.

Gansu regions to eastern Inner Mongolia (Fig. 1a and d).

Various hypotheses have emerged to elucidate the ascent of pastoralism around 3600 cal yr B.P. Some scholars posit that the emergence of pastoralism in North China stemmed from intercontinental cultural exchanges (Shao, 2004; Yang et al., 2019; Shao and Wu, 2020; Cong and Jia, 2020; Cao and Dong, 2020). Sheep and cattle, introduced to China before ~4000 cal yr B.P., subsequently underwent widespread domestication (Flad et al., 2007), paving the way for North China's pastoral transition. Another perspective relates the rise of pastoralism to climatic shifts (Yang, 1985; Qiao, 1992; Shao, 2004; Huang et al., 2004; Jia et al., 2016), contending that reduced precipitation and subsequent land degradation necessitated altered land-use strategies. A third standpoint underscores political factors (Wei et al., 2021; Shelach et al., 2003), proposing that frequent wars around 3600 cal yr B.P., stemming from Xia and Shang dynastic transitions (Xia-Shang-Zhou Chronology Project Expert Group, 2000), precipitated migrations as a defense against external threats.

Notably, the Northern Hemisphere witnessed cooling (Fig. 1b; Marcott et al., 2013) accompanied by decreased precipitation in the marginal monsoon areas of North China around 3600 cal yr B.P. For instance, xerophytic pollen proportions at the Zhukaigou site surged from 50% to 93% during the culture's latter phase (Han, 2005). The Huangqihai Lake's pollen data indicates the Holocene's driest epoch spanned 3600–3000 cal yr B.P. (Fig. 1c; Hao et al., 2014). Concurrently, archaeological findings reveal pastoral transitions primarily in ecologically vulnerable northern Chinese regions (Fig. 1d), areas oscillating between semi-humid and semi-arid conditions, characterized by forest and grassland. The climatic downturn around 3600 cal yr B.P. likely spurred desertification and agricultural declines in North China, compelling adaptive shifts to pastoralism. Nevertheless, agriculturally-centered cultures (e.g., Erlitou-Xinzhai, Yueshi, and Maqiao cultures) persisted in Central and South China post ~3600 cal yr B.P., even as notable cultural and climatic transitions occurred (Fig. 1d). Thus, climatic variations seemingly underpin North China's transition from cereal agriculture to pastoralism around 3600 cal yr B.P.

However, the specific attributes and dynamics of the ~3600 cal yr B.P. climate shift remain ambiguous. In this study, we probe the spatial configurations and causal mechanisms of this climatic transition by collating East Asian climate records spanning 4000–3000 cal yr B.P. Additionally, we elucidate potential links between the climate change, paleo-ENSO, and the rise of northern Chinese pastoralism around 3600 cal yr B.P.

## 2. Materials and methods

We compiled climate records from East Asia (Table 1), using the following selection criteria for this study:

1) Records must possess high resolution. They should span the period from 4000 to 3000 cal yr B.P., with a resolution better than 100 years, facilitating the effective discernment of centennial timescale climate shifts (Huang et al., 2023). In our dataset, two-thirds (20 of 33) of the climate records boast a resolution superior to 50 years.
2) Records must have detailed, high-precision, and high-resolution chronologies. Dating materials encompass stalagmites, tree rings, organic matter, and more. Employed dating methodologies include $^{230}$Th dating, radiocarbon dating, ring and varve counting, among others. The average age errors for $^{230}$Th dates (e.g., Li et al., 2014; Chen et al., 2021; Wang et al., 2022) and radiocarbon dates (e.g., Hao et al., 2014; Stebich et al., 2015; Chen et al., 2014; Ning et al., 2021) in this study were under 60 and 150 years, respectively. Moreover, most chosen records (22 of 33) feature over 10 dating points throughout the Holocene, with half of the records having over 12 dating points since 6000 cal yr B.P.

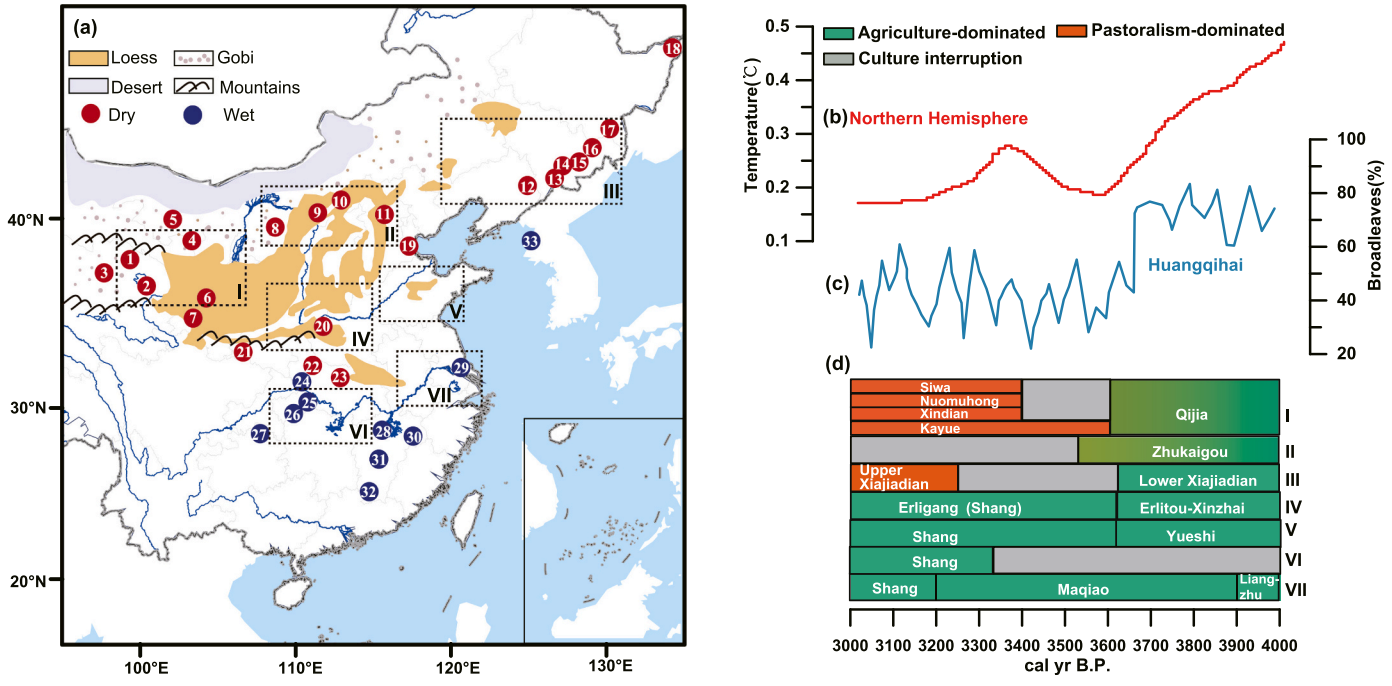



**Fig. 1.** (a) Locations of principal cultural regions (I–VII) in China (Liu and Feng, 2012) and referenced sites in the text. I: Gansu-Qinghai Cultural Region; II: Southern Inner Mongolia Cultural Region; III: Southeastern Inner Mongolia Cultural Region; IV: Central Plain Cultural Region; V: Haidai Cultural Region; VI: Middle Yangtze Cultural Region; VII: Lower Yangtze Cultural Region. Red (blue) dots denote sites where the climate transitioned from wet (dry) to dry (wet) around 3600 cal yr B.P. Comprehensive details of these sites are provided in Table 1. (b) Temperature record for the Northern Hemisphere (Marcott et al., 2013); (c) Pollen data from Huangqihai Lake, southern Inner Mongolia (Hao et al., 2014); (d) Cultural fluctuations in China between 4000 and 3000 cal yr B.P. (Han, 2005; Wang, 2012; Liu and Feng, 2012; Chen et al., 2015a; Dong et al., 2016; Chen et al., 2020; Shi et al., 2022). (For interpretation of the references to color in this figure legend, the reader is referred to the web version of this article.)

3) Proxies must reflect changes in humidity, precipitation, or temperature. The interpretations of the mentioned proxies are consistent with their original publications.
4) Sediments should be devoid of disturbances from human activities. Comprehensive details of these records are presented in Table 1.

While some records in Table 1 possess notable dating errors, we pinpointed the timing of the ~3600 cal yr B.P. climate transition using speleothem (e.g., Tan et al., 2020; Zhang et al., 2021a; Cai et al., 2021), tree-ring (Yang et al., 2021), and varved lake records (Zhou et al., 2010). These records, characterized by precise dating and high resolution (approximately five years), are frequently employed for reconstructing climate shifts on centennial and interdecadal scales (e.g., Tan et al., 2020; Huang et al., 2023).

## 3. Results and discussion

### 3.1. The ~3600 B.P. climate transition in China

Figs. 3 and 4 depict climate variations in China from 4000 to 3000 cal yr B.P. These figures highlight a contrasting trend in climate transition around 3600 cal yr B.P. between North and South China. In Northwest China (encompassing the Gansu-Qinghai Cultural Region shown in Fig. 1a), precipitation data reconstructed using glycerol dialkyl glycerol tetraethers from Hurleg Lake in the Qaidam Basin point to an arid shift since ~3600 cal yr B.P. (Zhang et al., 2023a). This shift is corroborated by increased aeolian activity in the region post ~3600 cal yr B.P. (Stauch, 2015). Tree-ring $\delta^{18}O$ record from Delingha in Qinghai province reveals that rainfall post ~3600 cal yr B.P. was notably reduced compared to prior levels (Fig. 3a; Yang et al., 2021). The proportion of tree pollen from Qinghai Lake also evidences a decline since ~3600 cal yr B.P. (Shen et al., 2005). Pollen data from Qingtu paleolake in Gansu province show a steppe desert dominated by *Artemisia* from 4300 to 3500 cal yr B.P., transitioning to a desert dominated by *Asteraceae* between 3500 and 3000 cal yr B.P., with the local environment evolving from a shallow lake to a marsh around 3500 cal yr B.P. (Zhao et al., 2008). The redness index from Tianchi Lake in Gansu province further supports an arid trend from ~3600 cal yr B.P. onwards (Fig. 3b; Zhou et al., 2010). The stalagmite $\delta^{13}C$ record from Wuya Cave in Gansu province suggests an arid trend starting around 3600 cal yr B.P. (Fig. 3c; Tan et al., 2020).

In southern Inner Mongolia (including the Southern Inner Mongolia Cultural Region shown in Fig. 1a), Baahar Nuur Lake on the Ordos Plateau vanished after ~3700 cal yr B.P. due to drier conditions (Guo et al., 2007). A rise in drought-resistant plants, such as *Ephedra*, from Aritonggutu Lake in the Badain Jaran Desert signifies a desert steppe landscape from ~3600 cal yr B.P., with peak aridity between 3600 and 800 cal yr B.P. (Ning et al., 2021). Pollen records from Daihai (Xiao et al., 2004; Xu et al., 2010) and Huangqihai (Fig. 3d; Hao et al., 2014) lakes demonstrate a pronounced drought trend around 3600 cal yr B.P., during which forests transitioned to shrublands. This is further corroborated by pollen data from Taishizhuang peatland in Hebei province (Tarasov et al., 2006).

In Northeast China (including the Southeastern Inner Mongolia

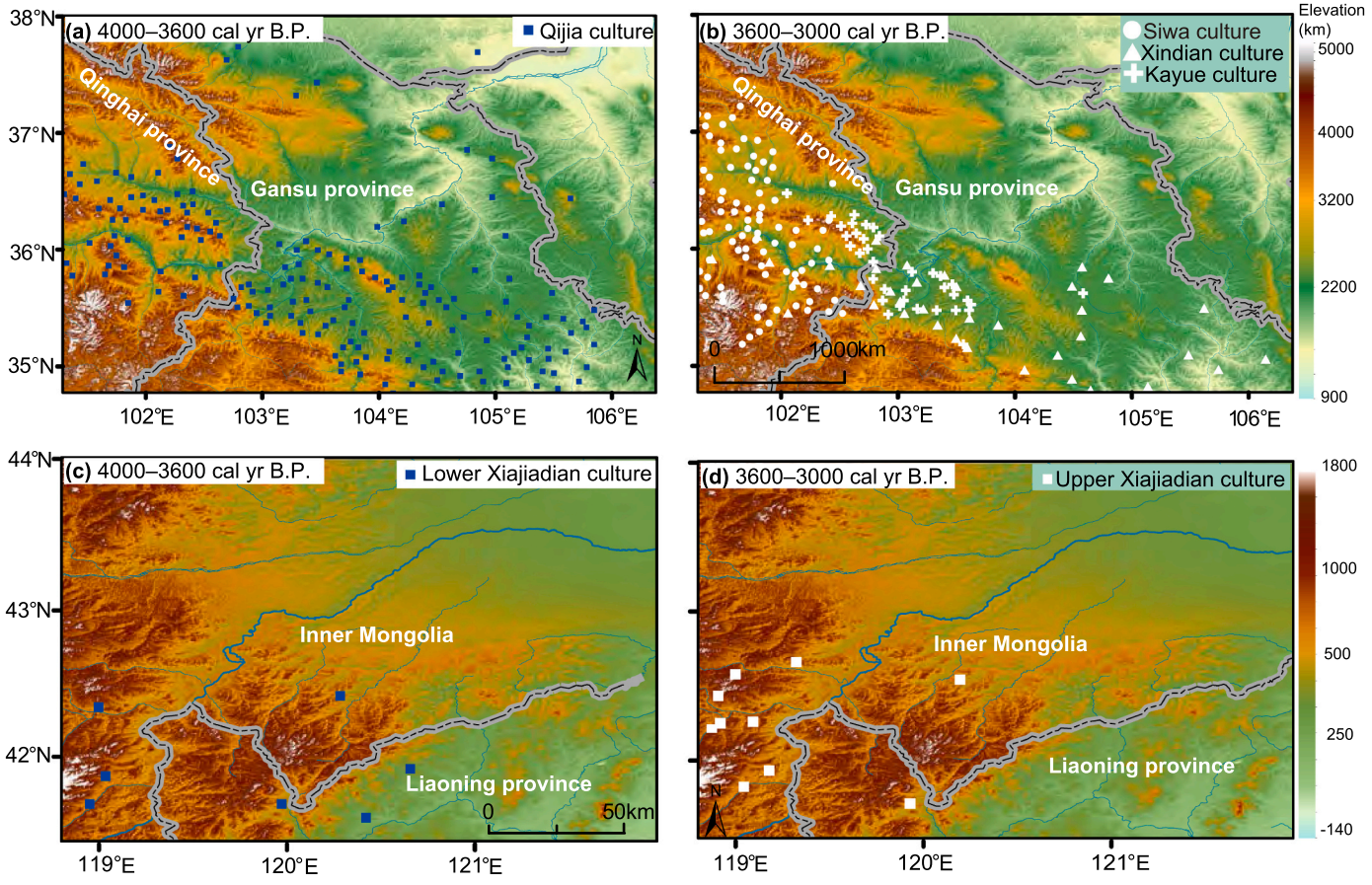



**Fig. 2.** Cultural shifts in North China around 3600 cal yr B.P. (Chinese Cultural Atlas Editorial Committee of National Cultural Heritage Administration, 2003, 2006, 2011; Xu et al., 2019). Culture distribution in the Gansu-Qinghai Cultural Region during (a) 4000–3600 cal yr B.P. and (b) 3600–3000 cal yr B.P. Culture distribution in the Southeastern Inner Mongolia Cultural Region for (c) 4000–3600 cal yr B.P. and (d) 3600–3000 cal yr B.P. Blue and white dots denote cereal agriculture and pastoralism, respectively. For the locations of these cultural regions, refer to Fig. 1a. (For interpretation of the references to color in this figure legend, the reader is referred to the web version of this article.)

**Table 1**
Detailed information for the climate records cited in the text.

| No. | Site | Lat. and Long. | Dating methods | Dating meterials | Dating num. | Time period | Sample resolution (yr) | Proxies used | Proxy indication | Reference |
|---|---|---|---|---|---|---|---|---|---|---|
| 1 | Delingha | 37°45′N, 97°67′E | Ring counting | Tree ring | – | 0–6700 | ~5 | $\delta^{18}O$ | Annual precipitation | Yang et al., 2021 |
| 2 | Qinghai Lake | 36°48′N, 100°08′E | $^{14}C$ | Organic matter | 10 | 0–18,000 | ~80 | Pollen | Vegetation; Humidity | Shen et al., 2005 |
| 3 | Hurleg Lake | 37°17′N, 96°55′E | $^{14}C$ | Organic matter | 4 | 0–14,000 | ~109 | Biomakers; Grain size | pH; Temperature; Precipitation | Zhang et al., 2023a |
| 4 | Qingtu paleolake | 39°04′N, 103°36′E | $^{14}C$ | Organic matter | 5 | 0–11,000 | ~57 | Pollen | Vegetation | Zhao et al., 2008 |
| 5 | Aritonggutu paleolake | 40°10′N, 102°18′E | $^{14}C$ | Pollen concentrates; Plant remains | 6 | 0–11,000 | ~47 | Pollen | Vegetation; Groundwater | Ning et al., 2021 |
| 6 | Tianchi | 35°15′N, 106°18′E | $^{14}C$ | Organic matter | 17 | 0–6200 | ~5 | Color; Pollen; Magnetic susceptibility | Vegetation; Humidity | Zhou et al., 2010 |
| 7 | Wuya Cave | 33°49′N, 105°26′E | $^{230}Th$ | Stalagmite | 29 | 0–6651 | ~5 | $\delta^{18}O$; $\delta^{13}C$ | Humidity | Tan et al., 2020 |
| 8 | Baahar Nuur Lake | 39°35′N, 109°19′E | $^{14}C$ | Organic matter | 16 | 3700–7700 | – | TOC, $\delta^{13}C$; Grain size; C/N | Humidity | Guo et al., 2007 |
| 9 | Daihai | 40°33′N, 112°39′E | $^{14}C$ | Organic matter | 8 | 0–10,000 | ~33 | Pollen | Precipitation; Vegetation | Xu et al., 2010 |
| 10 | Huangqihai Lake | 40°50′N, 113°17′E | $^{14}C$ | Organic matter | 6 | 0–8640 | ~52 | Pollen; TOC; C/N; TN; Grain size | Vegetation; Humidity | Hao et al., 2014 |
| 11 | Taishizhuang peatland | 40°24′N, 115°48′E | $^{14}C$ | Organic matter | 6 | 0–6000 | ~65 | Pollen | Vegetation; Humidity | Tarasov et al., 2006 |
| 12 | Nuanhe Cave | 41°20 N, 124°55′E | $^{230}Th$ | Stalagmite | 16 | 3400–10,500 | ~46 | $\delta^{18}O$ | Humidity | Wu et al., 2011 |
| 13 | Hani peatland | 42°13′N, 126°30′E | $^{14}C$ | Organic matter | 5 | 0–16,000 | ~45 | Grain size | Precipitation | Li et al., 2017 |
| 14 | Sihailongwan Maar Lake | 42°17'N, 126°36′E | Varve counting; $^{14}C$ | Plant remains | 40 | 0–12,000 | ~55 | Pollen | Precipitation; Temperature; Vegetation | Stebich et al., 2015 |
| 15 | Gushantun peatland | 42°18′N, 128°16′E | $^{14}C$ | Organic matter | 13 | 0–13,000 | ~17 | Pollen | Vegetation; Temperature; Precipiation | Leng, 2019 |
| 16 | Laolike peatland | 42°28′N, 128°39′E | $^{14}C$; $^{210}Pb$; $^{137}Cs$ | Plant remains | 24 | 0–12,100 | ~24 | $\delta^{13}C$; Grain size | Humidity | Dong et al., 2021 |
| 17 | Jingpo Lake | 43°59′N, 129°02′E | $^{14}C$ | Plant remains; Organic matter | 13 | 0–5100 | ~7 | TOC; TN; C/N; $\delta^{13}C$; Pollen | Vegetation; Humidity | Chen et al., 2014 |
| 18 | Heixiazi Island | 48°19′N, 134°44′E | $^{14}C$ | Plant remains; Organic matter | 7 | 0–9000 | ~90 | Pollen | Humidity | Zhang et al., 2020b |
| 19 | Haixing wetland | 37°56′N, 117°18′E | $^{14}C$ | Shell | 6 | 0–7600 | ~14 | Grain size; Geochemistry; Pollen; Algae | Humidity | Wang et al., 2023 |
| 20 | Magou Cave | 34°19'N, 113°23′E | $^{230}Th$ | Stalagmite | 10 | 0–85,000 | ~5.3 | $\delta^{13}C$; $\delta^{18}O$ | Local effective rainfall | Cai et al., 2021 |
| 21 | Xianglong Cave | 33°00′N, 106°20′E | $^{230}Th$ | Stalagmite | 33 | 1000–7000 | ~6 | Sr/Ca; $\delta^{18}O$; $\delta^{13}C$ | Local rainfall | Tan et al., 2018 |
| 22 | Xiniu Cave | 31°40′N, 110°25′E | $^{230}Th$ | Stalagmite | 14 | 0–13,000 | 4–10 | $\delta^{13}C$; $\delta^{18}O$ | East Asian summer monsoon | Zhang et al., 2020a |
| 23 | Yongxing Cave | 31°35'N, 114°14′E | $^{230}Th$ | Stalagmite | 7 | 3000–4400 | ~5.3 | $\delta^{13}C$ | Hydroclimatic variation | Zhang et al., 2023b |
| 24 | Dajiuhu peatland | 31°28′N, 109°59′E | $^{14}C$ | Plant remains | 10 | 0–16,000 | ~53 | Humification | Humidty | Ma et al., 2009 |
| 25 | Heshang Cave | 30°27′N, 110°25′E | $^{230}Th$ | Stalagmite | 21 | 0–9000 | ~16 | $\delta^{13}C_{ASOM}$ | Humidity; Temperature | Li et al., 2014 |
| 26 | Luoshui Cave | 29°44′N, 109°70′E | $^{230}Th$ | Stalagmite | 24 | 0–23,500 | ~9 | $\delta^{13}C$; $\delta^{18}O$ | Effective humidity | Wang et al., 2022 |
| 27 | Yangkou Cave | 29°02′N, 107°11′E | $^{230}Th$ | Stalagmite | 11 | 2920–5040 | ~7 | $\delta^{13}C$; $\delta^{18}O$ | Regional precipitation | Chen et al., 2021 |
| 28 | Poyang Lake | 29°20'N, 116°80′E | $^{14}C$ | Organic matter | 6 | 0–4000 | ~32 | Geochemistry | Weathering; Humidty | Huang et al., 2018 |
| 29 | Northern Yangtze Delta YZ07 | 32°50'N, 121°35′E | OSL | Quartz | 28 | 0–10,300 | ~219 | Pollen | Vegetation; Humidity | Ye et al., 2022 |
| 30 | Shennong Cave | 28°42′N, 117°15′E | $^{230}Th$ | Stalagmite | 52 | 1000–14,000 | ~100 | $\delta^{13}C$; $\delta^{18}O$ | Regional precipitation | Zhang et al., 2021b |

(*continued on next page*)

**Table 1** (*continued*)

| No. | Site | Lat. and Long. | Dating methods | Dating meterials | Dating num. | Time period | Sample resolution (yr) | Proxies used | Proxy indication | Reference |
|---|---|---|---|---|---|---|---|---|---|---|
| 31 | Jiulong Cave | 27°48′N, 113°54′E | $^{230}$Th | Stalagmite | 15 | 0–7000 | ~14 | $\delta^{13}C$; $\delta^{18}O$ | Regional precipitation | Zhang et al., 2021a |
| 32 | Dahu peatland | 24°15′N, 115°20′E | $^{14}$C | Organic matter | 17 | 0–18,000 | ~180 | TOC; Pollen | Humidity | Zhou et al., 2004 |
| 33 | South Korea | 39°51′N, 128°22′E | $^{14}$C | Organic matter | 17 | 0–9000 | ~11 | Zr; Ti; Si; Sr | Humidity | Lim et al., 2022 |

Cultural Region shown in Fig. 1a), the proportion of coarse silt and sand from the Hani peatland in Jilin province indicates a reduction in summer precipitation around 3600 cal yr B.P. (Li et al., 2017). Pollen-derived precipitation from the Sihailongwan Maar Lake (Fig. 3e; Stebich et al., 2015) and Gushantun (Leng, 2019) peatland in Jilin province exhibits a declining trend post ~3500 cal yr B.P. The $\delta^{13}C$ data from Laolike peatland in Jilin province also imply that Northeast China underwent a shift from a humid to an arid climate around 3600 cal yr B.P. (Dong et al., 2021). Multiple proxies (e.g., $\delta^{13}C$, grain size, pollen) from Jingpo Lake in Heilongjiang province highlight a humid phase from 5100 to 3600 cal yr B.P. and an arid phase from 3600 to 2100 cal yr B.P. (Fig. 3f; Chen et al., 2014). Pollen data from Heixiazi Island in Heilongjiang province reinforce the onset of arid conditions from ~3600 cal yr B.P. (Zhang et al., 2020b). Furthermore, an interruption in stalagmite growth within Nuanhe Cave in Liaoning province between 3500 and 2000 cal yr B.P. (Wu et al., 2011) implies that a dry climate interrupted the Karst process.

In Central China (encompassing the Central Plain and Haidai cultural regions shown in Fig. 1a), analyses such as geochemistry, grain size, pollen, and algae from the Haixing wetland in Hebei province suggest that the Bohai Bay sea level receded and the local environment became distinct from marine influences, pointing to a weakened monsoon around 3600 cal yr B.P. (Wang et al., 2023). Stalagmite $\delta^{13}C$ records from Magou Cave (Fig. 3g; Cai et al., 2021), Yongxing Cave (Zhang et al., 2023b), Xianglong Cave (Tan et al., 2018), and Xiniu Cave (Zhang et al., 2020a) all indicate an arid trend from ~3600 cal yr B.P. In summary, these records collectively demonstrate that North China transitioned from a humid to an arid climate around 3600 cal yr B.P.

However, the climate shift around 3600 cal yr B.P. in South China (encompassing the Middle and Lower Yangtze Cultural Regions as depicted in Fig. 1a) contrasts with that in North China. The speleothem $\delta^{13}C$ data from Luoshui Cave (Fig. 4a; Wang et al., 2022) and the $\delta^{13}C_{ASOM}$ record from Heshang Cave (Fig. 4b; Li et al., 2014) in Hubei province both suggest a humid trend from ~3600 cal yr B.P. Further, peat humification from Dajiuhu peatland in Hubei province points to a humid phase between 3700 and 3500 cal yr B.P. (Ma et al., 2009). In the northern Yangtze Delta, declining pollen percentages of *Artemisia* combined with an uptick in wetland herbs, freshwater algae, and coniferous forests (e.g., *Pinus*, Fig. 4c) hint at a moist period from 3400 to 1700 cal yr B.P. (Ye et al., 2022). The Ti/Na ratio (Fig. 4d) and the chemical index of alteration from Poyang Lake in Jiangxi Province infer wetter conditions post ~3500 cal yr B.P. (Huang et al., 2018). Speleothem $\delta^{13}C$ data from Jiulong Cave (Fig. 4e; Zhang et al., 2021a) and Shennong Cave in Jiangxi province (Zhang et al., 2021b), the $\delta^{13}C$ record from Yangkou Cave in Chongqing (Fig. 4f; Chen et al., 2021), and the total organic carbon data from Dahu peatland in Guangdong province (Zhou et al., 2004) collectively indicate that South China transitioned from an arid to a humid climate around 3600 cal yr B.P. A climate shift was also observed in South Korea, influenced by the Meiyu (literally plum rain), potentially connected to a rising frequency of typhoons across East Asia (Lim et al., 2022). Consequently, climatic patterns in North (north of 30°N) and South (south of 30°N) China highlight a meridional dipole pattern in the climate transition. This dipole transitioned from a "north wet–south dry" phase during 4000–3600 cal yr B.P. to a "north dry–south wet" phase between 3600 and 3000 cal yr B.P. (Fig. 1a).

### 3.2. The mechanism for the climate transition at ~3600 B.P

Meteorological studies indicate that the meridional precipitation gradient over East Asia can be influenced by ENSO, which modulates the location and intensity of the Western Pacific Subtropical High (Wang et al., 2000; Huang et al., 2012). During El Niño-like conditions, precipitation tends to decrease over North China but increase in South China (Ding and Chan, 2005; Huang et al., 2012). The pressing question is: Was the climatic shift around 3600 cal yr B.P. associated with variations in paleo-ENSO? In the eastern Pacific, both sand content (Conroy et al., 2008) and biomarker records (Fig. 5a; Zhang et al., 2014) from El Junco Lake, color data (Fig. 5b; Peterson et al., 2000) and Ti% findings (Haug et al., 2001) from the Cariaco Basin, and the color record from Laguna Pallcacocha (Fig. 5c; Moy et al., 2002) collectively indicate a shift toward a more El Niño-like state from ~3600 cal yr B.P. Furthermore, an El Niño-like condition also resulted in a cooling of thermocline water temperatures in the Indo-Pacific Warm Pool (Fig. 5d; Dang et al., 2012).

Given the simultaneous shifts in climate patterns over East Asia and the El Niño-like conditions in the tropical Pacific, we suggest that the emergence of an El Niño-like state may primarily drive the climate transition around 3600 cal yr B.P. Our findings establish that the interaction between paleo-ENSO and East Asian precipitation is evident not only on tectonic (Lu et al., 2021), orbital (Tian et al., 2022), sub-orbital (Chen et al., 2015b; Zhang et al., 2021d), and inter-decadal (Huang et al., 2012) scales but also at centennial scales. The Late Holocene's El Niño-like state in the tropical Pacific could be influenced by orbital forcings (e.g., Clement et al., 1999, 2000; Liu et al., 2014b). The decline in boreal summer insolation during the Late Holocene might generate zonally consistent sea surface temperature (SST) anomalies. However, the atmospheric response to these SST anomalies is more pronounced in the western Pacific compared to the eastern Pacific (Clement et al., 1999, 2000), resulting in more significant cooling of the atmosphere over the western Pacific and fostering El Niño-like conditions (Clement et al., 1999, 2000; Zhang et al., 2021c). The intensification of paleo-ENSO during the Late Holocene might also correlate with amplified positive ocean-atmosphere feedbacks driven by precession forcings (Liu et al., 2014b).

Beyond paleo-ENSO, the temperature decline over the Northern Hemisphere (Fig. 2b; Marcott et al., 2013) could also attenuate the East Asian summer monsoon and lead to a southward shift of the East Asian rain belt. This would yield decreased precipitation in North China and increased precipitation in South China (Zhang et al., 2023b). Consequently, the transition of the meridional dipole pattern around 3600 cal yr B.P. in China can be attributed to both a dominant El Niño-like state in the tropical Pacific and a temperature decrease in the Northern Hemisphere driven by insolation.

### 3.3. The El Niño-like-induced arid climate stimulates the rise of pastoralism in China

A growing body of evidence suggests a significant shift from cereal

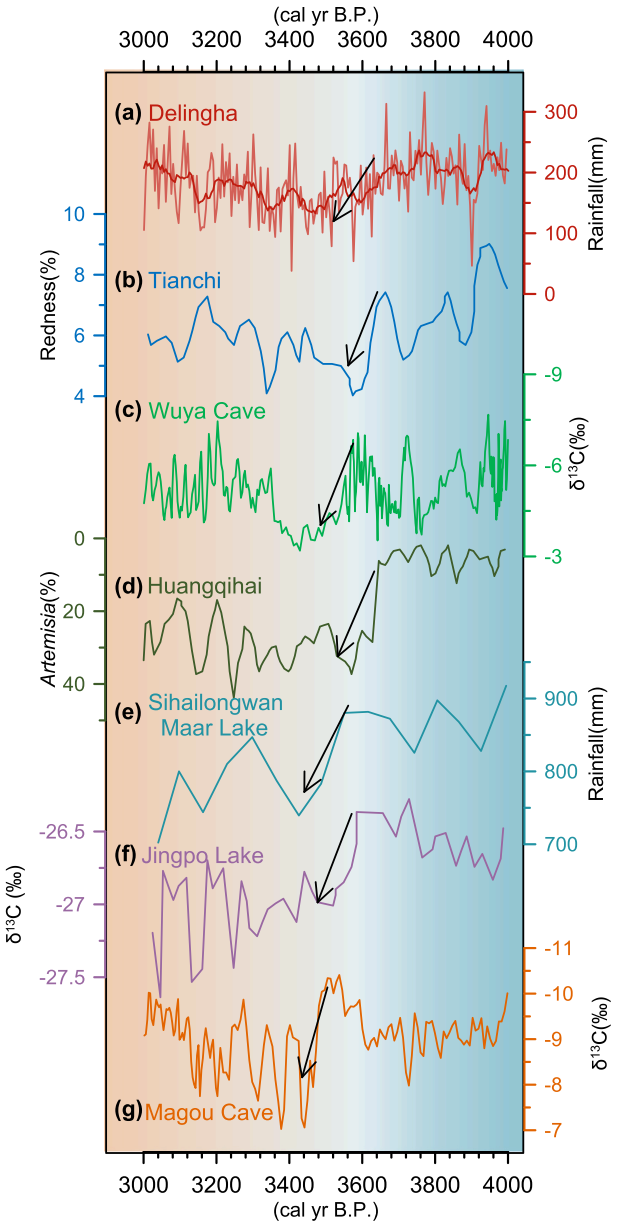



**Fig. 3.** Climate variations in North China from 4000 to 3000 cal yr B.P. (a) Annual (from the prior August to the current July) tree-ring $\delta^{18}O$ precipitation reconstruction at Delingha in Qinghai province (Yang et al., 2021); (b) Redness record from Tianchi Lake in Gansu province (Zhou et al., 2010); (c) Speleothem $\delta^{13}C$ record from Wuya Cave in Gansu province (Tan et al., 2020); (d) Pollen concentration of *Artemisia* from Huangqihai Lake in Inner Mongolia (Hao et al., 2014); (e) Precipitation reconstruction based on pollen from Sihailongwan Maar Lake in Jilin province (Stebich et al., 2015); (f) $\delta^{13}C$ record from Jingpo Lake in Heilongjiang province (Chen et al., 2014); (g) Speleothem $\delta^{13}C$ record from Magou Cave in Henan province (Cai et al., 2021). Blue and brown shading indicates humid and arid climates, respectively. (For interpretation of the references to color in this figure legend, the reader is referred to the web version of this article.)

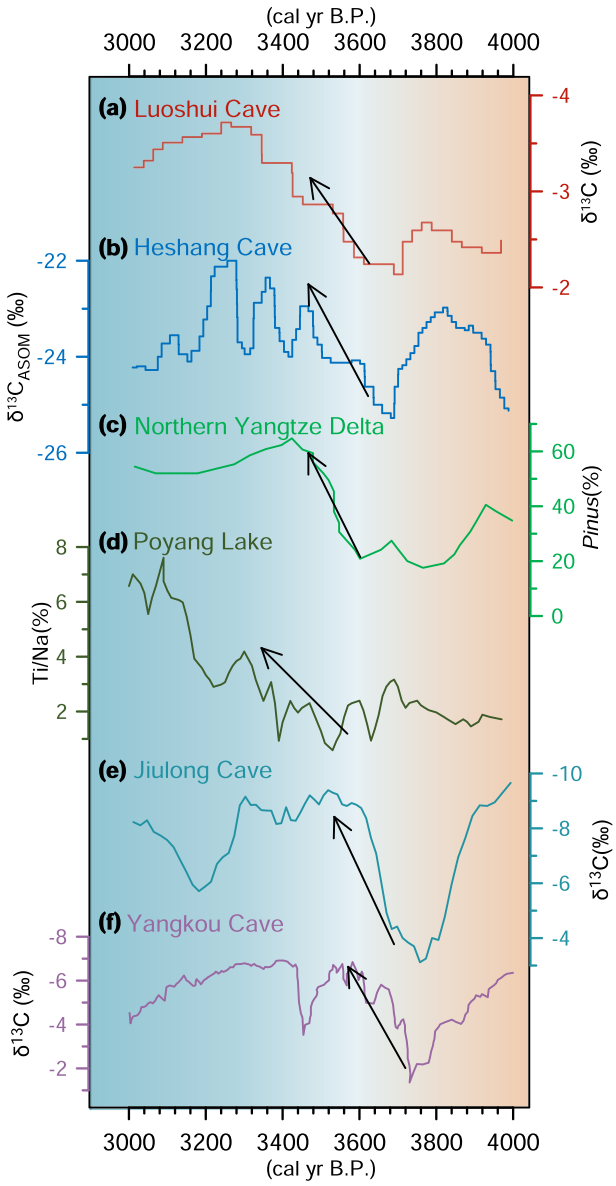



**Fig. 4.** Climate variations in South China from 4000 to 3000 cal yr B.P. (a) Speleothem $\delta^{13}C$ record from Luoshui Cave in Hubei province (Wang et al., 2022); (b) Speleothem $\delta^{13}C_{ASOM}$ record from Heshang Cave in Hubei province (Li et al., 2014); (c) Pollen concentration of Pinus in the northern Yangtze Delta (Ye et al., 2022); (d) Ti/Na record from Poyang Lake in Jiangxi province (Huang et al., 2018); (e) Speleothem $\delta^{13}C$ record from Jiulong Cave in Jiangxi Province (Zhang et al., 2021a); (f) Speleothem $\delta^{13}C$ record from Yangkou Cave in Chongqing (Chen et al., 2021). Blue and brown shading indicates humid and arid climates, respectively. (For interpretation of the references to color in this figure legend, the reader is referred to the web version of this article.)

agriculture to pastoralism around 3600 cal yr B.P. in the marginal monsoon areas (e.g., Chen et al., 2015a; Yang et al., 2019; Cao and Dong, 2020). Stable isotope analyses and zooarchaeological studies of faunal bones reveal an increased reliance on sheep and cattle herding in regions like the Hexi Corridor (Yang et al., 2019) and the Qinghai-Tibet Plateau post ~3600 cal yr B.P. (Chen et al., 2015a; Cao and Dong, 2020). Notably, bones of cattle and sheep constituted as much as 86.42% of identified samples in southeastern Inner Mongolia following this period (Shi et al., 2022). There was a substantial decline in millet seeds from the Lower Xiajiadian to the Upper Xiajiadian periods in the western Liao River Basin (Sun et al., 2014; Jia et al., 2016), with inhabitants showing a growing engagement in pastoralism (Jia et al., 2016).

Earlier research indicates that intercontinental cultural exchanges intensified around 3600 cal yr B.P. (e.g., Dodson et al., 2013; Liu et al., 2014a; Dong et al., 2016, 2017; Yang et al., 2019; Cao and Dong, 2020). Crops and technologies such as wheat, barley, and bronze, as well as animals like goats, sheep, cattle, and horses, were introduced to regions including the Hexi Corridor (Flad et al., 2007, 2010; Dodson et al., 2013; Liu et al., 2014a; Dong et al., 2016, 2017; Zhou et al., 2016; Yang et al., 2019), the Qinghai-Tibet Plateau (Chen et al., 2015a), and the Central

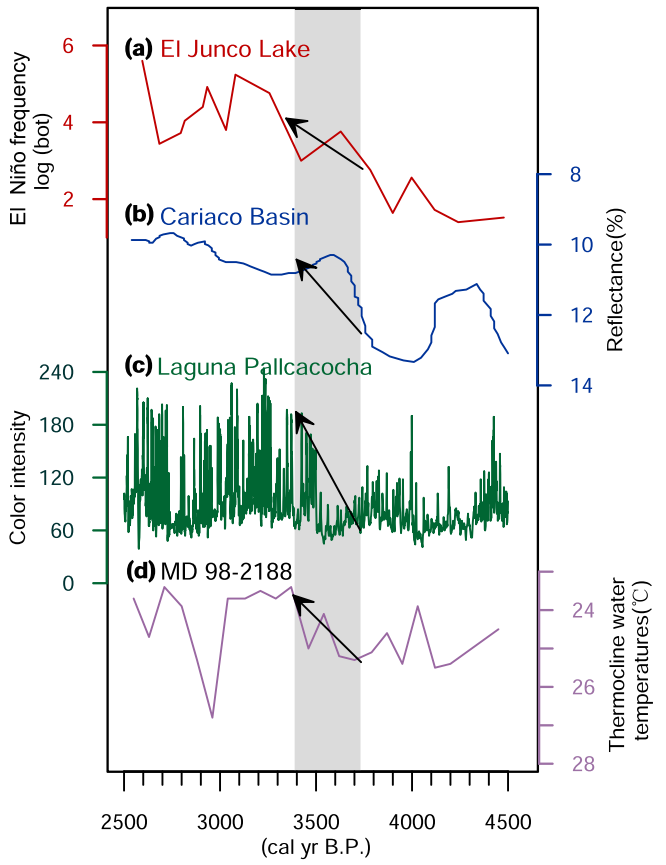



**Fig. 5.** Paleo-ENSO records from 5500 to 2500 cal yr B.P. (a) Biomarker record from El Junco Lake, San Cristobal, Galápagos (Zhang et al., 2014); (b) Color record from a deep-sea core in the Cariaco Basin (Peterson et al., 2000); (c) A 50-year running mean of grayscale intensity from a core in Laguna Pallcacocha, Ecuador (Moy et al., 2002); (d) Thermocline water temperature record from the MD 98–2188 in the Indo-Pacific Warm Pool (Dang et al., 2012).

Plains (Lee et al., 2007; Chen et al., 2015c). Concurrently, millet reached Central Asia around 3600 cal yr B.P. (Leipe et al., 2019). This surge in intercontinental exchanges facilitated technical innovations and reshaped local economies, driving the transition from cereal agriculture to pastoralism in North China (Yang et al., 2019; Cao and Dong, 2020).

However, besides the introduction of new food sources (e.g., cold-resistant crops and livestock) and technological advancements, the emergence of pastoralism was also influenced by climate change and regional characteristics (Han, 2005; Yang et al., 2019; Hu et al., 2022). For instance, while sheep, goats, and cattle were identified in the Central Plain (Chen et al., 2015c) and eastern Liaoning province (Shi et al., 2022) around 3600 cal yr B.P., regions dominated by agricultural practices persisted (Leipe et al., 2019; Tang et al., 2022). This underscores the possibility that climate played a significant role in the advent of pastoralism.

A pronounced El Niño-like state in the tropical Pacific around 3600 cal yr B.P. and a decline in temperature over the Northern Hemisphere (Marcott et al., 2013) led to significant drying in North China. Coupled with sustained farming from 4000 to 3600 cal yr B.P. (Zhou et al., 2012), this resulted in vegetation degradation and a reduction in arable land by ~3600 cal yr B.P. (Huang et al., 2004; Zhou et al., 2012, 2016). Consequently, the land in the marginal monsoon areas (e.g., Gansu-Qinghai region, southern and eastern Inner Mongolian regions) became unsuitable for rain-fed agriculture. Agricultural production decreased, putting the food supply at risk due to the worsening ecological environment (Huang et al., 2004; Ma et al., 2016). Notably, pastoralism requires less water compared to rain-fed agriculture (Madsen and Elston, 2007; Zhou et al., 2012). Thus, to sustain a large population, pastoralism supplanted cereal agriculture as the primary subsistence method in the marginal monsoon areas (Huang et al., 2004; Han, 2005; Zhou et al., 2012, 2016; Shi et al., 2022).

Indeed, climatic deterioration led to the diversification of food production during the Late Holocene (Chen et al., 2015a; Ma et al., 2016; Bevan et al., 2017; Yang et al., 2019). Alongside the rise of pastoral production, humans also adopted cold-resistant crops after ~3600 cal yr B.P. (e.g., Flad et al., 2010; Dodson et al., 2013; Liu et al., 2014a; Zhou et al., 2016). This shift is evidenced by changes in dietary patterns, with an increased intake of $C_3$ foods since ~3600 cal yr B.P. (Ma et al., 2016; Yang et al., 2019). Diverse subsistence strategies enhanced human adaptability to the colder and arid climate of the Late Holocene, facilitating human expansion to regions with harsher environments (Chen et al., 2015a; Jia et al., 2016; Dong et al., 2017; Yang et al., 2019; Cao and Dong, 2020). We recognize the significant influence of intercontinental cultural exchanges and other societal factors on the emergence of pastoralism in North China. However, we suggest that, against the backdrop of climate changes characterized by an El Niño-like state, survival pressures and amplified cultural exchanges across Eurasia created conditions favorable for the rise of pastoralism, ultimately driving the transition from cereal agriculture to pastoralism in North China.

## 4. Conclusions

The economy based on cereal agriculture shifted to one centered on pastoralism around 3600 cal yr B.P. in the marginal monsoon areas of North China, potentially due to climate change. This research investigates the underlying mechanisms of this climate transition around 3600 cal yr B.P. The findings reveal a change in China's meridional climate patterns: a "north wet (north of 30°N)–south dry (south of 30°N)" pattern prevailed from 4000 to 3600 cal yr B.P., but it reversed between 3600 and 3000 cal yr B.P. This climatic shift correlates with variations in the paleo-ENSO in the tropical Pacific. As the environment began deteriorating around 3600 cal yr B.P., humans transitioned from a sole reliance on cereal agriculture to an economy grounded in pastoralism. Given the broader context of societal progression, the environmental degradation in the marginal monsoon areas, driven by paleo-ENSO dynamics, catalyzed the emergence of pastoralism in North China by ~3600 cal yr B.P. Our research associates the variation in paleo-ENSO with the advent of pastoralism, underscoring the pivotal role of paleo-ENSO in the evolution of nomadic civilization.

## Declaration of Competing Interest

The authors declare that they have no known competing financial interests or personal relationships that could have appeared to influence the work reported in this paper.

## Data availability

Data will be made available on request.

## Acknowledgments

We are grateful to four anonymous reviewers for their thorough and valuable comments on an early version. This study was supported by the National Science Foundation of China (Grant no. 41830319) and the Strategic Priority Research Program of the Chinese Academy of Sciences (Grants: XDB26000000). Q.Z. Yin is Research Associate F.R.S.-FNRS.

## References


An, C.B., Tang, L.Y., Barton, L., Chen, F.H., 2005. Climate change and cultural response around 4000 cal yr B.P. In the western part of Chinese Loess Plateau. Quat. Res. 63, 347–352. https://doi.org/10.1016/j.yqres.2005.02.004.

Bevan, A., Colledge, S., Fuller, D., Fyfe, R., Shennan, S., Stevens, C., 2017. Holocene fluctuations in human population demonstrate repeated links to food production and climate. Proc. Natl. Acad. Sci. 114, E10524. https://doi.org/10.14324/000.ds.10025178.

Cai, Y.J., Cheng, X., Ma, L., Mao, R.X., Breitenbach, S.F., Zhang, H.W., Xue, G., Cheng, H., Edwards, R.L., An, Z.S., 2021. Holocene variability of East Asian summer monsoon as viewed from the speleothem $\delta^{18}O$ records in Central China. Earth Planet. Sci. Lett. 558, 116758 https://doi.org/10.1016/j.epsl.2021.116758.

Cao, H.H., Dong, G.H., 2020. Social development and living environment changes in the Northeast Tibetan Plateau and contiguous regions during the late prehistoric period. Region. Sustain. 1, 59–67. https://doi.org/10.1016/j.regsus.2020.09.001.

Chen, C.J., Yuan, X.D., Li, J.Y., Wang, X.F., Cheng, H., Ning, Y.F., Edwards, R.L., Wu, Y., Xiao, S.Y., Xu, Y.Z., Huang, Y.Y., Qiu, H.Y., Zhang, J., Liang, M.Q., Li, T.Y., 2021. The 4.2 ka event in East Asian monsoon region, precisely reconstructed by multi-proxies of stalagmite. In: Climate of the Past Discussions, p. 1. https://doi.org/10.5194/cp-2021-20.

Chen, J.H., Chen, F.H., Feng, S., Huang, W., Liu, J.B., Zhou, A.F., 2015b. Hydroclimatic changes in China and surroundings during the Medieval Climate Anomaly and Little Ice Age: spatial patterns and possible mechanisms. Quat. Sci. Rev. 107, 98–111. https://doi.org/10.1016/j.quascirev.2014.10.012.

Chen, R., Shen, J., Li, C.H., Zhang, E.L., Sun, W.W., Ji, M., 2014. Mid-to late-Holocene East Asian summer monsoon variability recorded in lacustrine sediments from Jingpo Lake, Northeastern China. The Holocene 25, 454–468. https://doi.org/10.1177/0959683614561888.

Chen, X.L., Fang, Y.M., Hu, Y.W., Hou, Y.F., Lü, P., Yuan, J., Song, G.D., Fuller, B.T., Richards, M.P., 2015c. Isotopic reconstruction of the late Longshan period (ca.4200-3900 BP) dietary complexity before the onset of state-level societies at the Wadian site in the Ying River valley, Central Plains,China. Int. J. Osteoarchaeol. 265, 808–817. https://doi.org/10.1002/oa.2482.

Chen, T.T., Qiu, M.H., Liu, R.L., Li, H.M., Hou, H.W., Howarth, P., Zhou, A.F., 2020. Human responses to climate change in the late prehistoric Western Loess Plateau, Northwest China. Radiocarbon 62, 1193–1207. https://doi.org/10.1017/RDC.2020.32.

Chen, F.H., Dong, G.H., Zhang, D.J., Liu, X.Y., Jia, X., An, C.B., Ma, M.M., Xie, Y.W., Barton, L., Ren, X.Y., Zhao, Z.J., Wu, X.H., Jones, M.K., 2015a. Agriculture facilitated permanent human occupation of the Tibetan Plateau after 3600 BP. Science 347, 248–250. https://doi.org/10.1126/science.1259172.

Chinese Cultural Atlas Editorial Committee of National Cultural Heritage Administration, 2003. Chinese Cultural Atlas-INNER MONGOLIA Volume. Xi'an Atlas Publisher Xi'an (in Chinese).

Chinese Cultural Atlas Editorial Committee of National Cultural Heritage Administration, 2006. Chinese Cultural Atlas-QINGHAI Volume. China Atlas Publisher, Beijing (in Chinese).

Chinese Cultural Atlas Editorial Committee of National Cultural Heritage Administration, 2011. Chinese Cultural Atlas-GANSU Volume. Surveying and Mapping Publisher, Beijing (in Chinese).

Clement, A.C., Seager, R., Cane, M.A., 1999. Orbital controls on the El Niño-Southern Oscillation and the tropical climate. Paleoceanography 14, 441–456. https://doi.org/10.1029/1999PA900013.

Clement, A.C., Seager, R., Cane, M.A., 2000. Suppression of El Niño during the mid-Holocene by changes in the Earth's orbit. Paleoceanography 15, 731–737. https://doi.org/10.1029/1999pa000466.

Cong, D.X., Jia, W.M., 2020. A review of prehistoric nomadic archaeological research on the Eurasian grasslands-from the perspective of prehistoric business models. The Western Regions Studies 4, 59–78 (in Chinese with English abstract).

Conroy, J.L., Overpeck, J.T., Cole, J.E., Shanahan, T.M., Steinitz-Kannan, M., 2008. Holocene changes in eastern tropical Pacific climate inferred from a Galápagos lake sediment record. Quat. Sci. Rev. 27, 1166–1180. https://doi.org/10.1016/j.quascirev.2008.02.015.

Cui, Y.F., Liu, Y.J., Ma, M.M., 2018. Spatiotemporal evolution of prehistoric Neolithic-Bronze Age settlements and influencing factors in the Guanting Basin, northeast Tibetan Plateau. Sci. China Earth Sci. 61, 149–162. https://doi.org/10.1007/s11430-017-9138-8.

Dang, H.W., Jian, Z.M., Bassinot, F., Qiao, P.J., Cheng, X.R., 2012. Decoupled Holocene variability in surface and thermocline water temperatures of the Indo-Pacific Warm Pool. Geophys. Res. Lett. 3, L01701. https://doi.org/10.1029/2011GL050154.

Ding, Y.H., Chan, J.C., 2005. The East Asian summer monsoon: an overview. Meteorol. Atmos. Phys. 89, 117–142. https://doi.org/10.1007/s00703-0050125-z.

Dodson, J.R., Li, X.Q., Zhou, X.Y., Zhao, K.L., Sun, N., Atahan, P., 2013. Origin and spread of wheat in China. Quat. Sci. Rev. 72, 108–111. https://doi.org/10.1016/j.quascirev.2013.04.021.

Dong, G.H., Ren, L.L., Jia, X., Liu, X.Y., Dong, S.M., Li, H.M., Wang, Z.X., Xiao, Y.M., Chen, F.H., 2016. Chronology and subsistence strategy of Nuomuhong culture in the Tibetan Plateau. Quat. Int. 426, 42–49. https://doi.org/10.1016/j.quaint.2016.02.031.

Dong, G.H., Yang, Y.S., Liu, X.Y., Li, H.M., Cui, Y.F., Wang, H., Chen, G.K., Dodson, J., Chen, F.H., 2017. Prehistoric trans-continental cultural exchange in the Hexi Corridor, Northwest China. The Holocene 28, 621–628. https://doi.org/10.1177/0959683617735585.

Dong, Y.M., Li, H.K., He, H.S., Wang, S.Z., 2021. Holocene peatland development, carbon accumulation and its response to climate forcing and local conditions in Laolike peatland, Northeast China. Quat. Sci. Rev. 268, 107124 https://doi.org/10.1016/j.quascirev.2021.107124.

Flad, R.K., Li, S.C., Wu, X.H., Zhao, Z.J., 2010. Early wheat in China: results from new studies at Donghuishan in the Hexi corridor. The Holocene 20, 955–965. https://doi.org/10.1177/0959683609358914.

Flad, R.K., Yuan, J., Li, S.C., 2007. Zooarcheological evidence for animal domestication in Northwest China. Dev. Quat. Sci. 9, 167–203. https://doi.org/10.1016/S1571-0866(07)09012-4.

Guo, L.L., Feng, Z.D., Li, X.Q., Liu, L.Y., Wang, L.X., 2007. Holocene climatic and environmental changes recorded in Baahar Nuur Lake core in the Ordos Plateau, Inner Mongolia of China. Chin. Sci. Bull. 52, 959–966. https://doi.org/10.1007/s11434-007-0132-1.

Han, M.L., 2005. The formation and climate change of the agricultural and pastoral interlaced zone in Northern China. Archaeology 10, 57–67 (in Chinese with English abstract).

Hao, Q., Liu, H.Y., Yin, Y., Wang, H.Y., Feng, M., 2014. Varied responses of forest at its distribution margin to Holocene monsoon development in northern China. Palaeogeogr. Palaeoclimatol. Palaeoecol. 409, 239–248. https://doi.org/10.1016/j.palaeo.2014.05.020.

Haug, G.H., Haughen, K.A., Sigman, D.M., Peterson, L.C., Roehl, U., 2001. Southward migration of the Intertropical Convergence Zone through the Holocene. Science 293, 1304–1308. https://doi.org/10.1126/science.1059725.

Hu, S.M., Yang, T., Yang, M.M., Shao, J., Di, N., 2022. Research on faunal remains from the Miaoliang site in Jingbian County, northern Shaanxi on the formation of animal husbandry in China. Quat. Sci. 42, 17–31. https://doi.org/10.11928/j.issn.1001-7410.2022.01.02 (in Chinese with English abstract).

Huang, C., Wei, G.J., Li, W.X., Liu, Y., 2018. A geochemical record of the link between chemical weathering and the East Asian summer monsoon during the late Holocene preserved in lacustrine sediments from Poyang Lake, Central China. J. Asian Earth Sci. 154, 17–25. https://doi.org/10.1016/j.jseaes.2017.12.008.

Huang, C.C., Pang, J., Zhou, Q., 2004. Holocene pedogenic change and the emergence and decline of rain-fed cereal agriculture on the Chinese Loess Plateau. Quat. Sci. Rev. 23, 2525–2535. https://doi.org/10.1016/j.quascirev.2004.06.003.

Huang, K.Y., Xie, D.H., Chen, C., Tang, Y.J., Wan, Q.C., Zhang, X., 2023. An environmental crisis and its cultural impact in eastern China around 6000 years ago. Palaeogeogr. Palaeoclimatol. Palaeoecol. 624, 111652 https://doi.org/10.1016/j.palaeo.2023.111652.

Huang, R., Chen, J., Wang, L., Lin, Z., 2012. Characteristics, processes, and causes of the spatio-temporal variabilities of the East Asian monsoon system. Adv. Atmos. Sci. 29, 910–942. https://doi.org/10.1007/s00376-012-2015-x.

Huang, X.Z., Liu, S.S., Dong, G.H., Qiang, M.R., Bai, Z.J., Zhao, Y., Chen, F.H., 2017. Early human impacts on vegetation on the northeastern Qinghai-Tibetan Plateau during the middle to late Holocene. Prog. Phys. Geogr. 41, 286–301. https://doi.org/10.1177/0309133317703035.

Jia, X., Sun, Y.G., Wang, L., Sun, W.F., Zhao, Z.J., Lee, H.F., Huang, W.B., Wu, S.Y., Lu, H.Y., 2016. The transition of human subsistence strategies in relation to climate change during the Bronze Age in the West Liao River Basin, Northeast China. The Holocene 26, 781–789. https://doi.org/10.1177/0959683615618262.

Lee, G.A., Crawford, G.W., Liu, L., Chen, X.C., 2007. Plants and people from the early neolithic to Shang periods in North China. Proc. Natl. Acad. Sci. 104, 1087–1092. https://doi.org/10.1073/pnas.0609763104.

Leng, 2019. Phytolith record of high-resolution climate change in Gushantun peatland since late glacial age. Northeast Normal University (in Chinese with English abstract).

Leipe, C., Long, T., Sergusheva, E.A., Wagner, M., Tarasov, P.E., 2019. Discontinuous spread of millet agriculture in eastern Asia and prehistoric population dynamics. Sci. Adv. 5, eaax6225. https://doi.org/10.1126/sciadv.aax6225.

Li, N.N., Chambers, F.M., Yang, J.X., Jie, D.M., Liu, L.D., Liu, H.Y., Gao, G.Z., Gao, Z., Li, D.H., Shi, J.C., Feng, Y.Y., Qiao, Z.H., 2017. Records of East Asian monsoon activities in Northeastern China since 15.6 ka, based on grain size analysis of peaty sediments in the Changbai Mountains. Quat. Int. 447, 158–169. https://doi.org/10.1016/j.quaint.2017.03.064.

Li, X.L., Hu, C.Y., Huang, J.H., Xie, S.C., Baker, A., 2014. A 9000-year carbon isotopic record of acid-soluble organic matter in a stalagmite from Heshang Cave, Central China: Paleoclimate implications. Chem. Geol. 388, 71–77. https://doi.org/10.1016/j.chemgeo.2014.08.029.

Lim, J., Um, I.K., Yi, S., Jun, C.P., 2022. Hydroclimate change and its controlling factors during the middle to late Holocene and possible 3.7 ka climatic shift over East Asia. Quat. Res. 109, 53–64. https://doi.org/10.1017/qua.2022.13.

Liu, F., Feng, Z., 2012. A dramatic climatic transition at ~4000 cal. yr BP and its cultural responses in chinese cultural domains. The Holocene 22, 1181–1197. https://doi.org/10.1177/0959683612441839.

Liu, X.Y., Lightfoot, E., O'Connell, T.C., Wang, H., Li, S.C., Zhou, L.P., Hu, Y., Motuzaite Matuzeviciute, G., Jones, M.K., 2014. From necessity to choice: dietary revolutions in West China in the second millennium BC. World Archaeol. 46, 661–680. https://doi.org/10.1080/00438243.2014.953706.

Liu, Z.Y., Lu, Z.Y., Wen, X.Y., Otto-Bliesner, B.L., Timmermann, A., Cobb, K.M., 2014. Evolution and forcing mechanisms of El Niño over the past 21,000 years. Nature 515, 550–553. https://doi.org/10.1038/nature13963.

Lu, J.Y., Yang, H., Griffiths, M.L., Burls, N.J., Xiao, G.Q., Yang, J.L., Wang, J.K., Johnson, K.R., Xie, S.C., 2021. Asian monsoon evolution linked to Pacific temperature gradients since the late Miocene. Earth Planet. Sci. Lett. 563, 116882 https://doi.org/10.1016/j.epsl.2021.116882.

Ma, C.M., Zhu, C., Zheng, C.G., Yin, Q., Zhao, Z.P., 2009. Climate changes in East China since the Late-glacial inferred from high-resolution mountain peat humification

records. Sci. China Earth Sci. 52, 118–131. https://doi.org/10.1007/s11430-009-0003-5.
Ma, M.M., Dong, G.H., Jia, X., Wang, H., Cui, Y.F., Chen, F.H., 2016. Dietary shift after 3600 cal yr BP and its influencing factors in northwestern China: evidence from stable isotopes. Quat. Sci. Rev. 145, 57–70. https://doi.org/10.1016/j.quascirev.2016.05.041.
Madsen, D.B., Elston, R.G., 2007. Variation in late Quaternary central Asian climates and the nature of human response. Dev. Quat. Sci. 9, 69–82. https://doi.org/10.1016/S1571-0866(07)09007-0.
Marcott, S.A., Shakun, J.D., Clark, P.U., Mix, A.C., 2013. A reconstruction of regional and global temperature for the past 11,300 years. Science 339, 1198–1201. https://doi.org/10.1126/science.1228026.
Moy, C.M., Seltzer, G.O., Rodbell, D.T., Anderson, D.M., 2002. Variability of El Niño/Southern Oscillation activity at millennial timescales during the Holocene epoch. Nature 420, 162–165. https://doi.org/10.1038/nature01194.
Ning, K., Wang, N.A., Yang, Z.J., Zhang, L.L., Wang, Y., Li, Z.L., Bi, Z.W., 2021. Holocene vegetation history and environmental changes inferred from pollen records of a groundwater recharge lake, Badain Jaran Desert, northwestern China. Palaeogeogr. Palaeoclimatol. Palaeoecol. 577, 110538 https://doi.org/10.1016/j.palaeo.2021.110538.
Peterson, L.C., Haug, G.H., Hughen, K.A., Rohl, U., 2000. Rapid changes in the hydrologic cycle of the tropical Atlantic during the last glacial. Science 290, 1947–1951. https://doi.org/10.1126/science.290.5498.1947.
Qiao, X.Q., 1992. Discussion on the origin of nomadic culture in northern China. Archaeol. Cultural Relics Inner Mongolia 1, 21–25 (in Chinese with English abstract).
Shao, F., 2004. Probing into the origin of nomadic industry in northern area of China. J. Renmin Univ. China 1, 144–149 (in Chinese with English abstract).
Shao, H.Q., Wu, Y.T., 2020. The research on the origin of early nomadism. Northern Cultural Relic 1, 28–37 (in Chinese with English abstract).
Shi, H.M., Jia, X., Wang, C., 2022. Zooarchaeology research at the Shuiquan site in Jianping County, Liaoning Province: Discussion of the utilization of animal remains along the Great Wall in North China around 4000 a B.P. Quat. Sci. 42, 32–46. https://doi.org/10.11928/j.issn.1001-7410.2022.01.0 (in Chinese with English abstract).
Shelach, G., Zhang, L., Yu, J., 2003. The rise of pastoral adaptation in Northeast China during the first Millennium BC: local processes and interregional interactions. Res. China's Front. Archaeol. 1, 237–262 (in Chinese with English abstract).
Shen, J., Liu, X.Q., Wang, S.M., Matsumoto, R., 2005. Palaeoclimatic changes in the Qinghai Lake area during the last 18,000 years. Quat. Int. 136, 131–140. https://doi.org/10.1016/j.quaint.2004.11.014.
Sun, Y.G., Zhao, Z.J., Cao, J.N., 2014. Analysis reportion flotation results of Erdaojingzi site in Inner Mongolian in 2009. Agric. Archaeol. 6, 1–9 (in Chinese with English abstract).
Stauch, G., 2015. Geomorphological and palaeoclimate dynamics recorded by the formation of aeolian archives on the Tibetan Plateau. Earth Sci. Rev. 150, 393–408. https://doi.org/10.1016/j.earscirev.2015.08.009.
Stebich, M., Rehfeld, K., Schlütz, F., Tarasov, P.E., Liu, J.Q., Mingram, J., 2015. Holocene vegetation and climate dynamics of NE China based on the pollen record from Sihailongwan Maar Lake. Quat. Sci. Rev. 124, 275–289. https://doi.org/10.1016/j.quascirev.2015.07.021.
Tan, L.C., Cai, Y.J., Cheng, H., Edwards, L.R., Gao, Y.L., Xu, H., Zhang, H.W., An, Z.S., 2018. Centennial- to decadal-scale monsoon precipitation variations in the upper Hanjiang River region, China over the past 6650 years. Earth Planet. Sci. Lett. 482, 580–590. https://doi.org/10.1016/j.epsl.2017.11.044.
Tan, L.C., Li, Y., Wang, X., Cai, Y.J., Lin, F., Cheng, H., Ma, L., Sinha, A., Edwards, R.L., 2020. Holocene monsoon change and abrupt events on the western Chinese Loess Plateau as revealed by accurately dated stalagmites. Geophys. Res. Lett. 46 https://doi.org/10.1029/2020GL090273 e2020GL090273.
Tang, L.Y., Zhang, Y., Zhu, J., Tian, J., Gao, X.P., Han, G.H., 2022. Study on the utilization of crops in Zhou Dynasty in the Zhengzhou region: a case from Guanzhuang site, Xingyang. Quat. Sci. 42, 129–143. https://doi.org/10.11928/j.issn.1001-7410.2022.01.11 (in Chinese with English abstract).
Tarasov, P., Jin, G., Wagner, M., 2006. Mid-Holocene environmental and human dynamics in northeastern China reconstructed from pollen and archaeological data. Palaeogeogr. Palaeoclimatol. Palaeoecol. 241, 284–300. https://doi.org/10.1016/j.palaeo.2006.03.038.
Tong, Z.C., 1993. The origin of the nomadic economy of the in northern China and a comparison of its material culture. Social Sci. Front 3, 188–195 (in Chinese with English abstract).
Tian, S.H., Dai, G.W., Yin, Q.Z., Meng, X.Q., Zhong, Z.S., Zhu, Z.M., Xiao, G.Q., 2022. Spatial differences in East asian climate transition at ~260 ka and their links to ENSO. Quat. Sci. Rev. 296, 107805 https://doi.org/10.1016/j.quascirev.2022.107805.
Wang, B., Wu, R., Fu, X., 2000. Pacific-East asian teleconnection: how does ENSO affect East asian climate? J. Clim. 13, 1517–1536. https://doi.org/10.1175/1520-0442(2000)013<1517:PEATHD>2.0.CO;2.
Wang, H., 2012. The lineage and pattern of neolithic and bronze age archaeological culture in Gansu and Qinghai. Archaeol. Res. 9, 210–243 (in Chinese with English abstract).
Wang, S.Y., Li, Y.C., Fan, B.S., Cao, Y.H., You, H.F., Wang, R.R., Ge, Y.W., Da, S.Q., She, Z.J., Zhang, Z., Zhang, S.R., Li, C.G., 2023. Middle to late Holocene environmental evolution and sea level change on the west coast of Bohai Bay. Quat. Int. https://doi.org/10.1016/j.quaint.2023.06.009 (in press).
Wang, Z.J., Chen, S.T., Wang, Y.J., Zhao, K., Liang, Y.J., Cheng, H., Shao, Q.F., Wang, X.F., Zhang, J.W., Wang, Q., Zhai, X.M., Edwards, R.L., 2022. A high-resolution stalagmite record from Luoshui Cave, Central China over the past 23.5 kyr. Quat. Sci. Rev. 282, 107443 https://doi.org/10.1016/j.quascirev.2022.107443.
Wei, H.C., Chongyi, E., Duan, R., Zhang, J., Sun, Y., Hou, G., Gao, J., 2021. Fungal spore record of pastoralism on the NE Qinghai-Tibetan Plateau since the middle Holocene. Sci. China Earth Sci. 64, 1318–1331. https://doi.org/10.1007/s11430-020-9787-4.
Wei, H.C., Chongyi, E., Zhang, J., Sun, Y.J., Li, Q.K., Hou, G.L., Duan, R.L., 2020. Climate change and anthropogenic activities in Qinghai Lake basin over the last 8,500 years derived from pollen and charcoal records in an Aeolian section. Catena 193, 104616. https://doi.org/10.1016/j.catena.2020.104616.
Wu, J., Wang, Y., Dong, J., 2011. Changes in East Asian summer monsoon during the Holocene recorded by stalagmite $\delta^{18}O$ records from Liaoning Province. Quat. Sci. 31, 990–998. https://doi.org/10.3969/j.issn.1001-7410.2011.06.06 (in Chinese with English abstract).
Xia-Shang-Zhou Chronology Project Expert Group, 2000. In: Report on the Xia-Shang-Zhou Chronology Project, 1996-2000 (simplified edition). World Publishing Co., Ltd, Beijing, pp. 1–56.
Xiao, J.L., Xu, Q.H., Toshio, N., Yang, X.L., Liang, W.D., Inouchi, Y., 2004. Holocene vegetation variation in the Daihai Lake region of north-Central China: a direct indication of the Asian monsoon climatic history. Quat. Sci. Rev. 23, 1669–1679. https://doi.org/10.1016/j.quascirev.2004.01.005.
Xie, D., 2002. Prehistoric Archaeology in Gansu-Qinghai. Cultural Relics Publishing House, Beijing (in Chinese).
Xu, D., Lu, H.Y., Chu, G.Q., Liu, L., Shen, C.M., Li, F.J., Wu, N.Q., 2019. Synchronous 500-year oscillations of monsoon climate and human activity in Northeast Asia. Nat. Commun. 10, 4105. https://doi.org/10.1038/s41467-019-12138-0.
Xu, Q.H., Xiao, J.L., Li, Y.C., Tian, F., Nakagawa, T., 2010. Pollen-based quantitative reconstruction of Holocene climate changes in the Daihai Lake area, Inner Mongolia, China. J. Climate 23, 2856–2868. https://doi.org/10.1175/2009JCLI3155.1.
Yang, B., Qin, C., Bräuning, A., Osborn, T.J., Trouet, V., Ljungqvist, F.C., Esper, J., Schneider, L., Grießinger, J., Büntgen, U., Rossi, S., Dong, G.H., Yan, M., Ning, L., Wang, J., Wang, X.F., Wang, S.M., Luterbacher, J., Cook, E.R., Stenseth, N.C., 2021. Long-term decrease in asian monsoon rainfall and abrupt climate change events over the past 6,700 years. Proc. Natl. Acad. Sci. U. S. A. 18, e2102007118 https://doi.org/10.1073/pnas.2102007118.
Yang, Y., 1985. Further understanding of the first social division of labor: a study of the diversity of the origin and development of agriculture and animal husbandry in China from archaeological discoveries. J. Anhui Normal Univ. (Human. Social Sci. Ed.) 3, 37–44 (in Chinese with English abstract).
Yang, Y.S., Ren, L.L., Dong, G.H., Cui, R., Liu, G., Chen, H., Wang, S., Wilken, S., Chen, F.H., 2019. Economic change in the prehistoric Hexi Corridor (4800–2200 BP), north-West China. Archaeometry 61, 957–976. https://doi.org/10.1111/arcm.12464.
Ye, L.T., Gao, L., Li, Y.F., Wang, G.Q., 2022. Palynology-based reconstruction of Holocene environmental history in the northern Yangtze Delta,China, 603, 111186. https://doi.org/10.1016/j.palaeo.2022.111186.
Zhao, Y., Yu, Z., Chen, F., Li, J., 2008. Holocene vegetation and climate change from a lake sediment record in the Tengger Sandy Desert, northwest China. J. arid environ. 72, 2054–2064. https://doi.org/10.1016/j.jaridenv.2008.06.016.
Zhang, W., Chen, S.T., Shao, Q.F., Chen, J.S., 2023b. Hydroclimatic variation over Central China during the 4.2 ka event and its implications for cultural transformation. Palaeogeogr. Palaeoclimatol. Palaeoecol. 615, 111441 https://doi.org/10.1016/j.palaeo.2023.111441.
Zhang, H.W., Cheng, H., Sinha, A., Spötl, C., Cai, Y.J., Liu, B., Kathayat, G., Li, H.Y., Tian, Y., Li, Y.W., Zhao, J.Y., Sha, L.J., Lu, J.Y., Meng, B.L., Niu, X.W., Dong, X.Y., Liang, Z.Y., Zong, B.Y., Ning, Y.F., Lan, J.H., Edwards, R.L., 2021a. Collapse of the Liangzhu and other Neolithic cultures in the lower Yangtze region in response to climate change. Sci. Adv. 7, eabi9275. https://doi.org/10.1126/sciadv.abi9275.
Zhang, T., Wang, G., Wang, Y.L., Wei, Z.F., He, W., Ma, X.Y., Ma, H., Yu, X.L., Zhang, P.Y., Li, S.K., Wei, J.Y., Li, L., 2023a. Long-term drying trends since the mid-Holocene in the Qaidam Basin. Catena 228, 107145. https://doi.org/10.1016/j.catena.2023.107145.
Zhang, S., Yu, Z.F., Gong, X., Wang, Y., Chang, F.M., Lohmman, G., Li, T.G., Li, Q.Y., 2021c. Precession cycles of the El Niño/Southern oscillation-like system controlled by Pacific upper-ocean stratification. Commun. Earth Environ. 2, 239. https://doi.org/10.1038/s43247-021-00305-5.
Zhang, H.W., Zhang, X., Cai, Y.J., Sinha, A., Spotl, C., Baker, J., Kathayat, G., Liu, Z.Y., Tian, Y., Lu, J.Y., Wang, Z.Q., Zhao, J.Y., Jia, X.X., Du, W.J., Ning, Y.F., An, Z.S., Edwards, R.L., Cheng, H., 2021b. A data-model comparison pinpoints Holocene spatiotemporal pattern of East asian summer monsoon. Quat. Sci. Rev. 261, 106911 https://doi.org/10.1016/j.quascirev.2021.106911.
Zhang, Z.Q., Bianchette, T.A., Meng, C.H., Xu, Q.H., Jiang, M., 2020b. Holocene vegetation-hydrology-climate interactions of wetlands on the Heixiazi Island,China. Sci. Total Environ. 743, 140777 https://doi.org/10.1016/j.scitotenv.2020.140777.
Zhang, W.C., Dodson, J., Chang, M.X., Li, G.X., 2021d. Hydrological changes related to ENSO-like states during the last deglaciation in central eastern China. Paleoceanogr. Paleoclimatol. 36, PA004279. https://doi.org/10.1029/2021PA004279.
Zhang, J.W., Kong, X.G., Zhao, K., Wang, Y.J., Liu, S.H., Wang, Z.J., Liu, J.W., Cheng, H., Edwards, R.L., 2020a. Centennial-scale climatic changes in Central China during the Holocene climatic optimum. Palaeogeogr. Palaeoclimatol. Palaeoecol. 558, 109950 https://doi.org/10.1016/j.palaeo.2020.109950.
Zhang, Z.H., Leduc, G., Sachs, J.P., 2014. El Niño evolution during the Holocene revealed by a biomarker rain gauge in the Galápagos Islands. Earth Planet. Sci. Lett. 404, 420–434. https://doi.org/10.1016/j.epsl.2014.07.013.
Zhou, A.F., Sun, H.L., Chen, F.H., Zhao, Y., An, C.B., Dong, G.H., Wang, Z.L., Chen, J.H., 2010. High-resolution climate change in mid-late Holocene on Tianchi Lake, Liupan Mountain in the Loess Plateau in Central China and its significance. Chin. Sci. Bull. 55, 2118–2121. https://doi.org/10.1007/s11434-010-3226-0.

Zhou, W.J., Yu, X.F., Timothy Jull, A.J., Burr, G., Xiao, J.L., Lu, X.F., Xian, F., 2004. High-resolution evidence from southern China of an early Holocene optimum and a mid-Holocene dry event during the past 18,000 years. Quat. Res. 62, 39–48. https://doi.org/10.1016/j.yqres.2004.05.004.

Zhou, X.Y., Li, X.Q., Dodson, J., Zhao, K.L., 2016. Rapid agricultural transformation in the prehistoric Hexi corridor,China. Quat. Int. 426, 33–41. https://doi.org/10.1016/j.quaint.2016.04.021.

Zhou, X.Y., Li, X.Q., Dodson, J., Zhao, K.L., Atahan, P., Nan, S., Yang, Q., 2012. Land degradation during the Bronze Age in Hexi Corridor (Gansu, China). Quat. Int. 254, 42–48. https://doi.org/10.1016/j.quaint.2011.06.046.